THE PROTEIN SOCIETY

Conformational stability of CopC and roles of residues Tyr79 and Trp83

Zhen Song, Xiaoyan Zheng, and Binsheng Yang*

Institute of Molecular Science, Key Laboratory of Chemical Biology and Molecular Engineering of Ministry of Education, Shanxi University, Taiyuan, China 030006

Received 20 May 2013; Revised 10 August 2013; Accepted 13 August 2013
DOI: 10.1002/pro.2338
Published online 21 August 2013 proteinscience.org

Abstract: CopC is a periplasmic copper Chaperone protein that has a β-barrel fold and two metal-binding sites distinct for Cu(II) and Cu(I). In the article, four mutants (Y79F, Y79W, Y79WW83L, Y79WW83F) were obtained by site-directed mutagenesis. The far-UV CD spectra of the proteins were similar, suggesting that mutations did not bring any significant changes in secondary structures. Meanwhile the effects of mutations on the protein's function were manifested by Cu(II) binding. Fluorescence lifetime measurement and quenching of tryptophan fluorescence by acrylamide and KI showed that the microenvironment around Trp83 was more hydrophobic than that around Tyr79 in apoCopC. Unfolding experiments induced by guanidinium chloride (GdnHCl), urea provided the conformational stability of each protein. The $\Delta<\Delta G^0_{element}>$ obtained using the model of structural elements was used to show the role of Tyr79 and Trp83. On the one hand, the $<\Delta G^0_{element}>$ induced by urea for Y79F, Y79W have a loss of 6.51, 2.03 kJ/mol, respectively, compared with apoCopC, proving that replacement of Tyr79 by Phe or Trp all decreased the protein stability, meaning that the hydrogen bonds interactions between Tyr79 and Thr75 played an important role in stabilizing apoCopC. On the other hand, the $<\Delta G^0_{element}>$ induced by urea for Y79WW83L have a loss of 11.44 kJ/mol, but for Y79WW83F did a raise of 1.82 kJ/mol compared with Y79W. The replacement of Trp83 by Phe and Leu yields opposite effects on protein stability, which suggested that the aromatic ring of Trp83 was important in maintaining the hydrophobic core of apoCopC.

Keywords: conformational stability; unfolding of CopC; hydrogen bond; hydrophobic packing

Introduction

Proteins carry out the most important tasks in living organisms.[1] To perform such tasks, most proteins fold to a globular conformation, which is essential for their biological functions. These folded conformations are more stable than unfolded, biologically inactive conformations under physiological conditions.[2] This small net conformational stability is the result of much larger contributions from several important forces in which the major stabilizing forces are hydrogen bonding and hydrophobic effect.

Intramolecular hydrogen bonds are essential to the structure and stability of globular proteins. In an unfolded protein, most polar groups are hydrogen bonded to and partially surrounded by water molecules. In a folded protein, most polar groups form one or more intramolecular hydrogen bonds and surrounded by polar and nonpolar groups that make up the interior of a folded protein.[3] A native protein molecule is folded

Abbreviations: CD, circular dichroism; GdnHCl, guanidinium hydrochloride; Leu, leucine; Phe, Phenylalanine; Tyr, Tyrosine; Thr, threonine; Trp, tryptophan; Y79F/Y79W, The two single mutants of apoCopC in which the tyrosine(Y) residue has been replaced by phenylalanine (F), tryptophan (W), respectively; Y79WW83L/Y79WW83F, The two double mutants of apoCopC, in which the tyrosine(Y) residue has been replaced by tryptophan (W) and the tryptophan (W) has been replaced by leucine (L), phenylalanine (F), respectively.

Additional Supporting Information may be found in the online version of this article.

Grant sponsor: the National Natural Science Foundation of PR China; Grant number: 20771068 and 20901048. Grant sponsor: PhD Programs Foundation of the Ministry of Education of China; Grant number: 20091401110007. Grant sponsor: Natural Science Foundation Shanxi Province; Grant number: 2007011024.

*Correspondence to: Yang, Binsheng, Institute of Molecular Science, Key Laboratory of Chemical Biology and Molecular Engineering of Ministry of Education, Shanxi University, Taiyuan, China 030006. E-mail: yangbs@sxu.edu.cnss)

into a uniquely defined configuration held by hydrogen bonds. The importance of the hydrogen bond in protein structure can hardly be overemphasized.[4]

A classic review by Kauzmann[5] firmly shifted the emphasis from hydrogen bonding and convinced most protein chemists that globular proteins are stabilized mainly by hydrophobic bonding. The stability of native conformation in water can be explained entirely based on the hydrophobic interactions of the nonpolar parts of the molecule fostered by Tanford.[6] The initial efforts to use site-directed mutagenesis to investigate the forces that stabilize proteins focused on hydrophobic effect.[7]

Aromatic side chains such as tryptophan (Trp), tyrosine (Tyr), and phenylalanine (Phe) have a unique role in the protein folding. Given that these aromatic side chains are among the most hydrophobic, they are important in hydrophobic clustering.[8] Furthermore, Trp, Phe, and Tyr may be conserved to ensure the structural stability of folding.[9] A common but unique feature of most Greek key proteins is the "tyrosine corner." Four Greek key proteins have been reported to possess "tryptophan corners," where Trp replaces the Tyr residue. As a consequence of its high conservation, the tyrosine corner has been postulated to be important in the folding and/or stabilization of native protein.[10] In addition, the aromatic amino acid Trp is the intrinsic fluorescent probe most widely used for monitoring protein conformational changes, dynamics, and intermolecular interactions due to its indole chromophore, which is very sensitive to its environment.[11]

The CopC protein has been proposed to be a copper chaperone protein consisting of 102 amino acids.[12] Copper is one of the most prevalent transition metals in living organisms, but is also very toxic in free form because of its ability to produce radicals by cycling between oxidized Cu(II) and reduced Cu(I).[13] Thus, maintaining appropriate nutritional levels is very important. Copper chaperones are the kind of proteins that guide and protect the copper ion within the cell, delivering it safely to the appropriate functional protein receptors.[14,15] CopC has high affinity distinct for Cu(I) and Cu(II),[16–19] and the solution structure of Cu(II)-CopC from *Pseudomonas Syringae* has been obtained.[20] However, the binding sites of CopC can also be occupied by other transition metal ions, although the affinity is lower than that of copper ions. For example, Hg(II) ions can bind to both sites,[21] whereas Ag(I) only binds to the Cu(I) site.[22] Research suggests that cis-$Pt(NH_3)_2Cl_2$ (cisplatin) occupies the Cu(I) site, specifically in the 1:1 Pt–CopC adducts.[23]

The stability of small globular proteins is a problem that is of outmost interest in biochemistry and biophysics, as demonstrated in the literature.[24] In this study, we sought to further characterize the conformational differences induced by mutation. Chemical denaturation is a method that allows for measurement and comparison of protein stabilities,[25] wherein differences in the slope, transition midpoints, and overall shape of the unfolding curves signify structural differences among proteins. This study reports on guanidinum ion (GdnHCl), as well as urea unfolding studies of apoCopC and its mutations monitored by fluorescence spectroscopy. Four CopC variants are used to explore the roles of Trp83 and Tyr79 on protein stability. These unfolding curves are fitted with two and three states to generate free-energy values that describe the protein stabilities. The results suggest that the hydrogen bond interactions between Tyr79 and Thr75 as well as the interactions between the aromatic ring of Trp83 and other residues have an important role in stabilizing apoCopC. The differences in microenvironment around the two important resides are interpreted based on the quenching experiments and fluorescence lifetime measurement results. These findings demonstrate that the microenvironment around Trp83 is more hydrophobic than that around Tyr79 in apoCopC.

Results

Effects of mutations on the conformations of apoCopC

As shown in Figure 1, folded CopC (apoCopC and various mutants) exhibits a negative CD signal around 210 to 220 nm, which is a characteristic of the β-sheet structure. The far-UV CD spectra of these five proteins are similar, suggesting that the four mutations did not give rise to any significant changes in the secondary structures. Although the protein structure did not undergo major changes, the subtle changes should be analyzed. The data from CD revealed that the β-sheet content (Y79F, Y79W) was reduced by 11 and 8% compared with apoCopC, respectively [Fig. 1(A)]. Similarly, the β-sheet content for Y79WW83L exhibited a loss of 5%, whereas that for Y79WW83F increased by 2% compared with Y79W, as shown in Figure 1(B).

Emission fluorescence spectra

To assess the effect of the mutation on the fluorescence characteristics of the protein, we analyzed their emission spectra using fluorescence spectroscopy. Mutant proteins showed a subtle shift in emission wavelength, suggesting that the polarity of the microenvironment around the Trp changed a little, but were still hydrophobic. As shown in Figure 2(A), the emission maximum of Y79W was 325 nm and that of Y79F was 320 nm. For Y79WW83L and Y79WW83F, as shown in Figure 2(B), the emission maximums were 331 and 328 nm, respectively. For apoCopC and Y79F, the only Trp was located at the 83 position. However, for Y79WW83L and

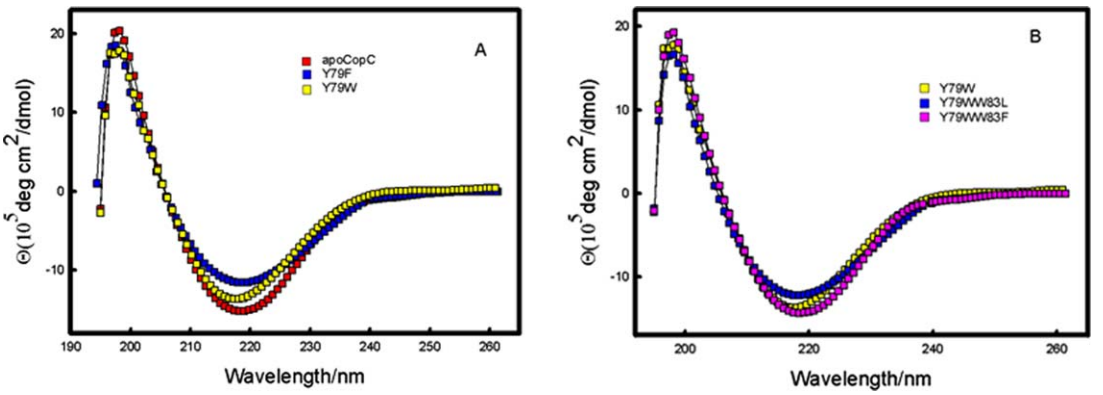

Figure 1. Far-UV CD spectra of protein (25 μ*M*) (A: apoCopC, Y79F, and Y79W) (B: Y79W, Y79WW83L, and Y79WW83F) using 1-mm path length quartz cells in 2 m*M* Hepes, pH 7.4, at 25°C. [Color figure can be viewed in the online issue, which is available at wileyonlinelibrary.com.]

Y79WW83F, the only Trp was located at the 79 position. The fluorescence parameters of Trp residues are sensitive to the environment (environment-sensitive fluorophores). The emission maximum of the Trp fluorescence spectrum depends on the properties of the environment around Trp residues in proteins. The explanation was that the microenvironment around Trp83 was different from that around Tyr79.

Effects of mutations on the binding capacity of Cu(II)

The apoCopC protein is a small soluble molecule (10.5 kDa) with a β-barrel structure; it features two distinct copper-binding sites that are highly specific for Cu(I) and Cu(II). To explore the effects of mutations on the protein function, an experiment on the proteins combined with copper was carried out. Titration of proteins with Cu(II) quenched the fluorescence intensity linearly until 1 equiv of Cu(II) was bound, as shown in Figure 3(A). The fluorescence intensity decreased by 60% for Y79F and apoCopC. However, the intensity decreased by 40% for Y79WW83L and Y79WW83F, suggesting that the fluorescence was quenched by Cu(II) in a large degree when the Trp in the protein was located at the 83 position. This result may be due to the fact that copper-binding sites located at the N-terminal and Trp83 were closer to the copper-binding sites than Trp79. Job's plot is shown in Figure 3(B), in which the fluorescence intensity at 320 nm decreased linearly in two slopes, and the stoichiometry of Cu(II) binding with Y79F was 1:1. When [Cu(II)]/([Cu(II)]+[Y79F]) <0.5, fluorescence intensity was observed from the free Y79F and Cu(II)-Y79F. However, when [Cu(II)]/([Cu(II)]+[Y79F]) ≥ 0.5, the fluorescence intensity was only observed from Cu(II)-Y79F, and the content of Cu(II)-Y79F decreased with the reduction in the concentration of Y79F.

To calculate the binding constants between Cu(II) and mutants, we used EDTA as a competitive ligand. The fluorescence intensity (*F*) values at 320 nm were derived from the titration of Y79F with EDTA-Cu(II), and the titration curves were prepared by plotting F versus [Cu(II)] [Fig. 3(C)]. Assuming that the decrease in fluorescence intensity at given

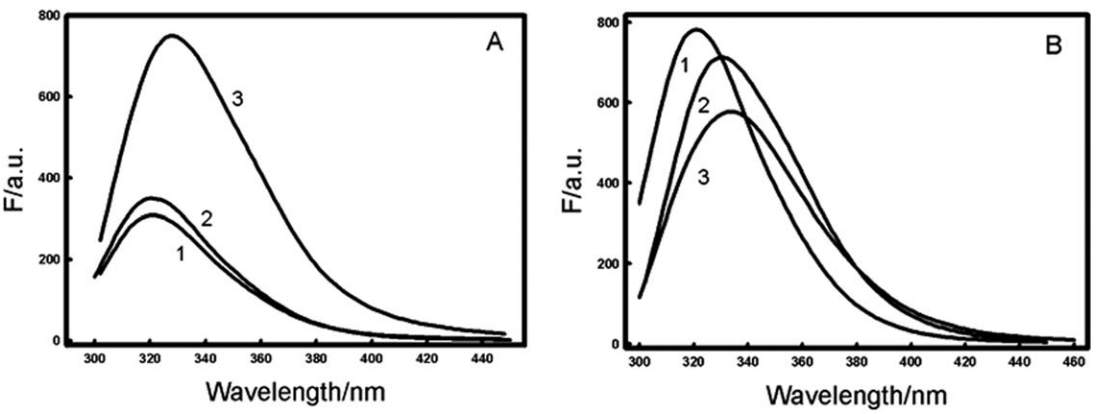

Figure 2. The emission fluorescence spectra (A: apoCopC (1), Y79F (2) and Y79W (3)). (B: apoCopC (1), Y79WW83F (2) and Y79WW83L (3)), excited at 295 nm in 10 m*M* Hepes, pH 7.4, at 25°C.

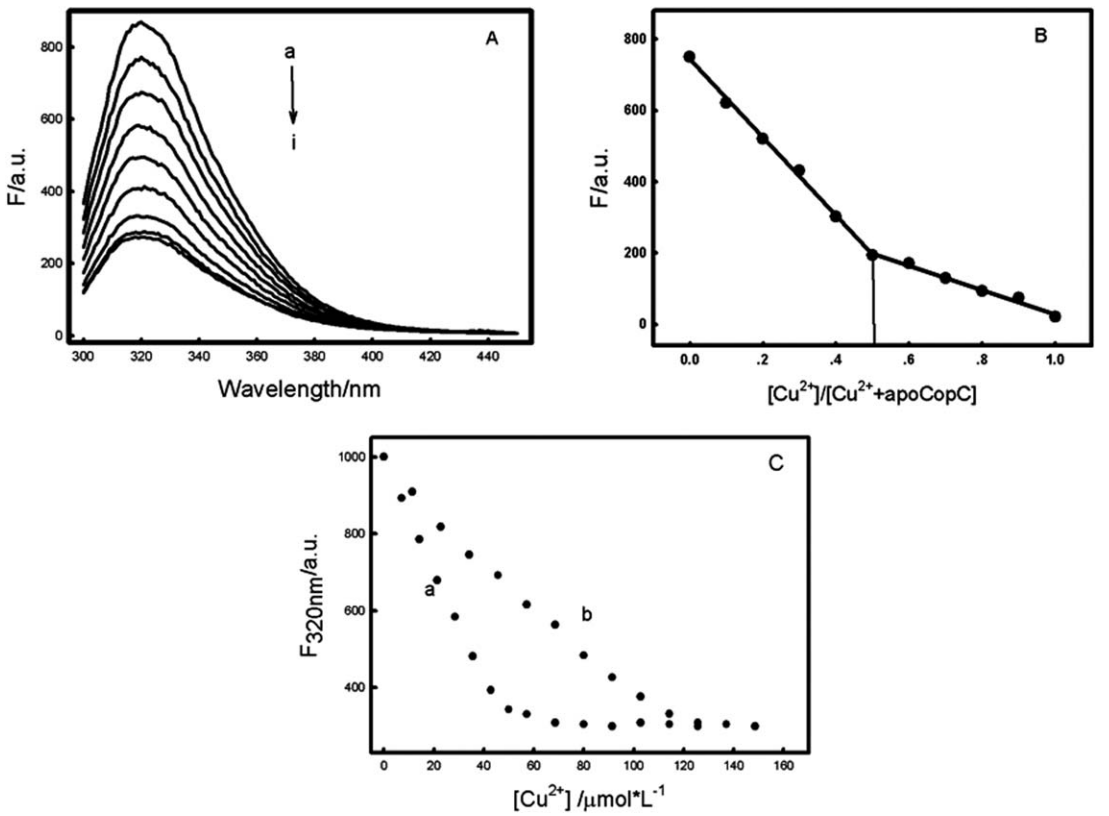

Figure 3. A: The fluorescence spectra of Y79F (50 μ*M*) at different concentrations of Cu(II) in 10 m*M* Hepes, pH 7.4, at 25°C. The concentration of Cu^{2+} from a to i is 0, 7, 14, 21, 28, 35, 42, 49, 60 μ*M*, respectively. B: Job's plot of fluorescence intensity at 320 nm against [Cu(II)]/([Cu(II)]+[Y79F]) in 10 m*M* Hepes, pH 7.4, at 25°C. The sum concentration of Y79F and Cu(II) is 2.0×10^{-6}*M* and [Cu(II)]/([Cu(II)]+[Y79F]) is 0, 0.1, 0.2, 0.3, 0.4, 0.5, 0.6, 0.7, 0.8, 0.9, and 1.0, respectively. C: The titration curve of Y79F by Cu(II) (a) or Cu(II)-EDTA (1:0.5) (b).

[Cu(II)] is attributed to the change of Cu(II)-Y79F to Cu(II)-EDTA, the binding constant can be calculated with Formulas (1) to (7) (See Supporting Information). The constants of the other mutants can be obtained through the same method. The binding constants of Cu(II) and proteins are listed in Table I. The data showed that the binding ability of Cu(II) was not affected by mutations.

Fluorescence lifetimes of apoCopC and its mutants

Investigating the intrinsic fluorescence from protein is an effective method to study protein conformational dynamics. CopC has a single Trp residue, so it has been studied using a single Trp residue as an intrinsic fluorophore. The indole double ring has a dual physical nature. This ring has a great hydrophobic van der Waals surface area, but possesses a highly polar NH group. For the "exposed" tryptophyls, the most preferable situation is that where indole is partly buried by its benzol ring and interacts with water through its NH group. According to the model proposed by Burstein,[27] the fluorescence properties of the Trp residues in the proteins suggest the existence of three discrete spectral classes: one buried in the nonpolar regions of the protein (λ_{em} = 330–332 nm, τ = 2.1 ns) and two on the surface. One of the latter is completely exposed to water (λ_{em} = 350–353 nm, τ = 5.4 ns), whereas the other is in limited contact with water, which is probably immobilized by bonding at the macromolecular surface (λ_{em} = 340–342 nm, τ = 4.4 ns). Fluorescence decays of CopC and its mutants in 10 m*M* Hepes, pH 7.4, at 25°C are shown in Figure 4. Figure 4(A) shows the decays of apoCopC, Y79F, and Y79W, wherein their lifetimes were different, although the fluorescence spectrum for Y79F was the same as that for apoCopC. Similarly, Figure 4(B) shows the decays of apoCopC, Y79WW83L, and Y79WW83F. The lifetimes of Y79WW83L and Y79WW83F were larger than that of apoCopC. For apoCopC, the single Trp was located at the 83 position, whereas the single Trp for Y79WW83L and Y79WW83F was

Table I. *The Binding Constants of Cu(II) and Proteins*

Protein	K (M^{-1})	R^2
apoCopC	$(2.24 \pm 0.36) \times 10^{14}$	0.97
Y79F	$(0.19 \pm 0.04) \times 10^{14}$	0.94
Y79W	$(1.53 \pm 0.16) \times 10^{14}$	0.98
Y79WW83L	$(0.31 \pm 0.03) \times 10^{14}$	0.98
Y79WW83F	$(0.28 \pm 0.42) \times 10^{14}$	0.96

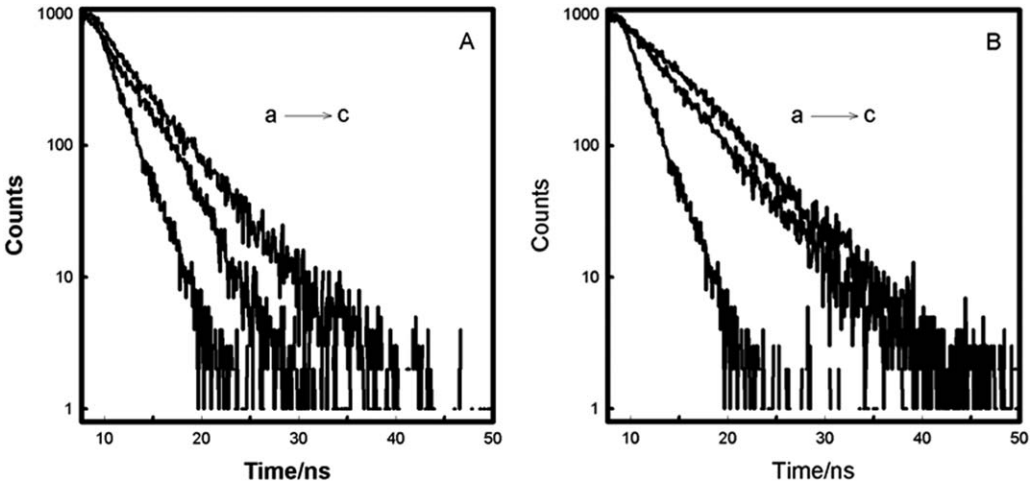

Figure 4. Fluorescence decays of [A: apoCopC (a), Y79F (b), and Y79W (c)]. [B: ApoCopC (a), Y79WW83F (b), and Y79WW83L (c)] in 10 m*M* Hepes, pH 7.4, at 25°C.

located at the 79 position. In other words, the lifetimes of Trp in proteins increase in a manner dependent on the position of the Trp residue. From the lifetime values listed in Table II, we posit that the exposed degree of Tyr79 in a hydrophilic environment is more enhanced compared with that of Trp83. The results coincided with the data from the fluorescence emission spectra. Y79W has two lifetimes, suggesting that the environments around these two Trp residues are different. One residue was located in a hydrophobic environment, whereas the other was located at a relatively hydrophilic environment.

Acrylamide and KI quenching

Fluorescence quenchers are widely used in studying the relative accessibilities of fluorescent groups in proteins. KI and acrylamide are the universal quenching agents. Acrylamide quenching is very sensitive to the degree of Trp accessibility to the solvent containing the acrylamide. Given that acrylamide can diffuse into the interior of the protein, accessibility to acrylamide may result from the existence of channels leading to the interior of the protein. Iodide ion is hydrated and is limited by its large size and charge to quenching of Trp residues lying at or near the surface of proteins.[28] Quenching of the protein Trp fluorescence by KI involves a collision-quenching mechanism.[29] Eftink and Ghiron[30] reported that K_{SV} derived from the slope of the Stern–Volmer plot, can, in effect, be taken as a crude estimation of the accessibility of Trp residues in proteins. Stern–Volmer plots for the KI quenching of proteins fluorescence, with fluorescence emission monitored at 320 nm, are shown in Figure 5(A). Parallel quenching experiments were performed with acrylamide, a polar, uncharged water-soluble molecule that can penetrate a protein matrix as a function of protein size and dynamics.[31] The linear Stern–Volmer plots of F_0/F versus acrylamide concentration are shown in Figure 5(B). The quenching parameter analyses obtained from the Stern–Volmer plots are presented in Table III. The data list in Table III reveals that the degree quenched by acrylamide is significantly greater than that of KI. This phenomenon suggests that Trp is buried in the protein deeply, and acrylamide, a neutral quencher, can access Trp easily. Furthermore, the quenched degree for the Trp located at 79 was larger than that located at 83, which is in agreement with the conclusion derived from KI.

GdnHCl/urea-induced unfolding of apoCopC and its mutants

A denaturant refers to a reagent that decreases the stability of protein and leads to a structural change from its specific, compact, and three-dimensional structure to an unfolded state. From the structural point of view, urea and GdnHCl are very similar but the latter is a positive ion. Therefore, we can surmise that GdnHCl, giving rise to charged species in water, could effectively interfere with favorable electrostatic interactions among the charged groups on the protein surface. The molecular mechanisms of GdnHCl and urea denaturation are different[32–36] and the screening of favorable electrostatic

Table II. *The Fluorescence Parameters of apoCopC and Its Mutants*

Protein	Amplitude (B_i)	Lifetime, τ_i (ns)	χ^2
apoCopC	0.092	1.85	1.079
Y79F	0.065	3.69	1.018
Y79W	0.040, 0.043	1.67, 4.65	1.060
Y79WW83L	0.055	5.19	1.117
Y79WW83F	0.063	4.72	1.079

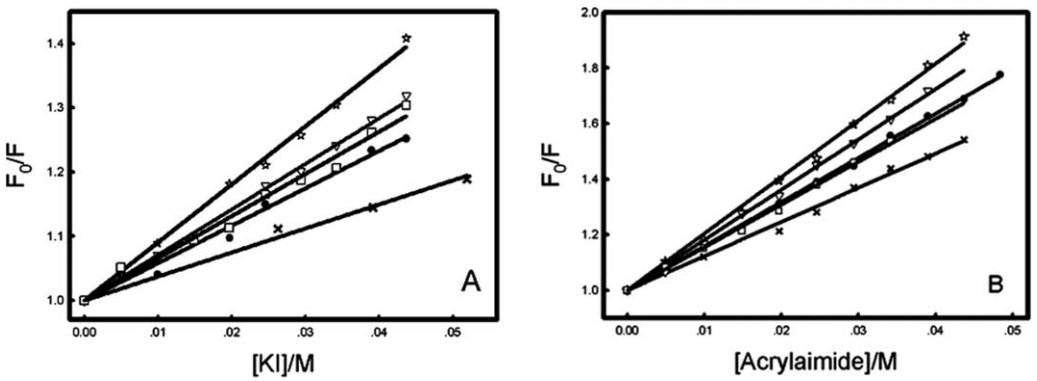

Figure 5. Stern–Volmer plots of iodide (A) and acrylamide (B) quenching of apoCopC (x), Y79W (☆), Y79F (●), Y79WW83F (□), and Y79WW83L (▽) in 10 m*M* Hepes, pH 7.4, at 25°C.

interactions on the surface of globular proteins may be the only real difference between the two denaturants.

The thermodynamic stability of apoCopC and its mutants was tested in GdnHCl/urea-induced unfolding experiments in 10 m*M* Hepes, pH 7.4, at 25°C. In proteins, Trp is highly sensitive to the polarity of its surrounding environment. Native apoCopC exhibited an maximum emission at 320 nm. In 3*M* GdnHCl, the spectra remained similar in shape, but the emission maximum peak shifted from 320 to 350 nm, which corresponds to the fluorescence maximum of Trp in an aqueous solution. The fluorescence spectra of Y79F under different concentrations of GdnHCl are shown in Supporting Information Figure S1. To best assess the shape of the apoCopC transitions, a ratio of fluorescence intensities at 400 and 310 nm ($I_{400\ nm}/I_{310\ nm}$) was plotted as a function of denaturant concentration. At low denaturant concentration, the unfolding fraction was 0, indicating that the protein was in the fold state. The unfolding fraction increased with the further denaturant accumulation. When the concentration reached a certain value, the unfolding fraction was 1 and the protein unfolded completely. The unfolding curves of the mutants were obtained through the same method. As shown in Figure 6(A), the unfolding curves of Y79F, Y79W, and apoCopC were similar, and the unfolding transitions best fitted to a two-state model, the unfolding–transition midpoints for Y79F and Y79W shifted to lower GdnHCl concentrations. The data listed in Table V show that the stabilities of Y79F and Y79W decreased, and Y79F was less stable compared with Y79W. The corresponding urea-unfolding experiments are shown in Figure 6(B). Similarly, the unfolding of Y79F and apoCopC was the same as above, confirming the two-state processes. Notably, the unfolding of the Y79W mutant induced by urea best fitted to a three-state model. A tiny plateau was present in the transition region from 6 to 6.2*M* urea, suggesting greater population of the partially folded intermediate within the scope of urea concentration. Equilibrium unfolding data obeyed a three state model with midpoints of 4.6 and 7.1*M* urea for the first and second transitions, respectively. According to the structure element model, the unfolding curve of Y79W can be fitted by the combination of Y^1 and Y^2 (see analysis of denaturation data in Supporting Information Fig. S2). The thermodynamics parameters of the unfolding of proteins induced by urea and GdnHCl are listed in Tables IV and V, respectively.

Table III. Stern–*Volmer Constants of apoCopC and Its Mutants Using Different Quenchers*

	K_{SV} (M^{-1})	
Protein	Acrylamide	KI
apoCopC	12.45 ± 0.36	3.62 ± 0.24
Y79F	15.91 ± 0.19	6.12 ± 0.28
Y79W	20.83 ± 0.34	9.15 ± 0.20
Y79WW83F	15.61 ± 0.36	6.54 ± 0.12
Y79WW83L	18.53 ± 0.29	7.31 ± 0.27

Figure 6(C,D) was obtained using the methods of Figure 6(A,B). By contrast, the unfolding curve of Y79W was added in Figure 6(C,D), in which the unfolding of Y79WW83L best fitted to the two-state model induced by urea or GdnHCl. The two state fit unfolding curves yielded midpoints of 0.64*M* GdnHCl and 3*M* urea for Y79WW83L [Fig. 6(C,D)]. The midpoint of transition for Y79WW83L was much less than that for Y79W. Interestingly, the unfolding experiments with Y79WW83F revealed some differences. The unfolding curves obtained for Y79WW83F seemed to involve two sequential transitions (see analysis of denaturation data in Supporting Information Figs. S3 and S4). This result indicates that the equilibrium–unfolding reactions have three states. The GdnHCl-induced unfolding curve of Y79WW83F showed that the midpoint of the first transition was 1.16*M*, whereas that of the second transition was 1.54*M* GdnHCl [Fig. 6(C)]. Similar to GdnHCl, the unfolding transition induced by urea had three states, with a transition midpoint

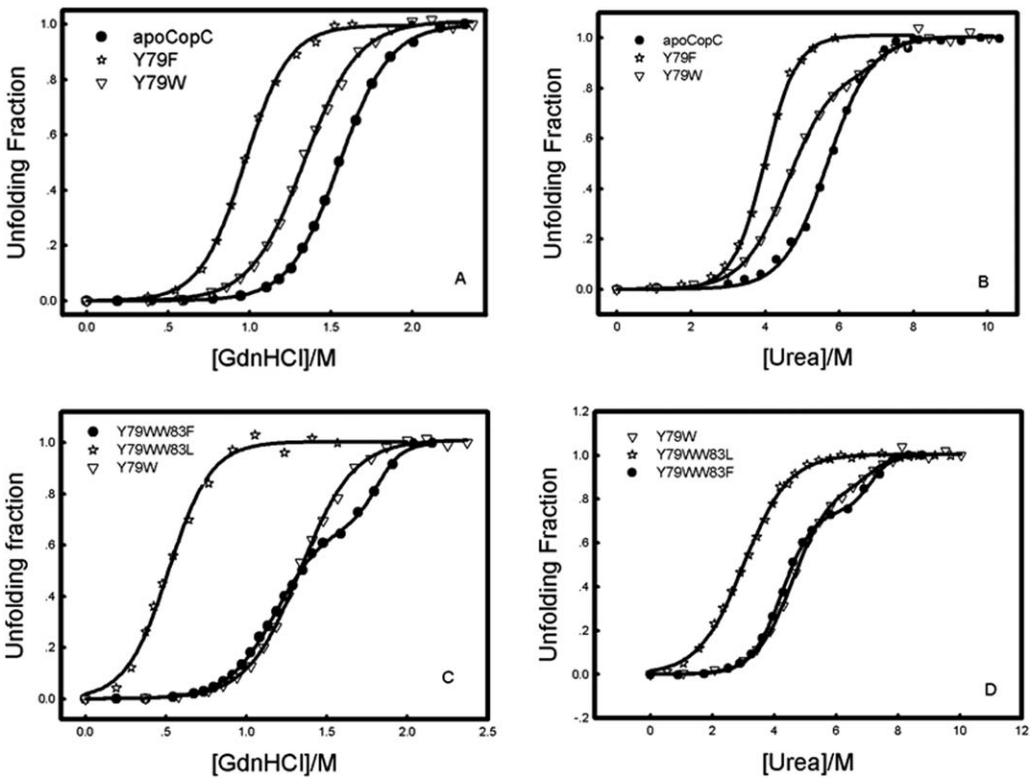

Figure 6. GdnHCl (A and C) or urea (B and D) induced unfolding of apoCopC and its mutants. Denaturation of protein was monitored by fluorescence spectroscopy. Samples of a fixed concentration of protein (2 μ*M*) were titrated with GdnHCl from 0 to 3*M* and were allowed to unfold for 30 min at 25°C before the measurement of fluorescence intensity. The unfolding experiment induced by urea was carried under the same condition.

of 4.2*M* urea for the transition from native to intermediate and a midpoint of 7.2*M* urea for the intermediate to the unfolded transition [Fig. 6(D)]. The thermodynamics parameters of the unfolding of proteins induced by urea and GdnHCl are listed in Tables IV and V, respectively.

Figure 6 and Tables IV and V show that the stabilities of apoCopC, Y79W, and Y79F followed the series apoCopC>Y79W>Y79F. The difference among these three proteins was only the 79th amine acid. The abilities of the formation of hydrogen bonds decreased successively, which revealed that the ability of the 79th amine acid to form H-bonds has an important role in maintaining the structure of apoCopC. The stabilities of Y79W, Y79WW83L, and Y79WW83F followed the series Y79WW83F>Y

Table IV. *Thermodynamics Parameters of apoCopC and Its Mutants from Urea-Induced Unfolding at pH 7.4, 25°C*

	Protein	Parameters	F (I/U)	I (U)	$\langle\Delta G^0_{element}\rangle$ (kJ/mol)	$\Delta\langle\Delta G^0_{element}\rangle$ (kJ/mol)
	apoCopC	$[D]_{1/2}$ (M)	5.68			
		$-m$ (kJ/M/mol)	4.36 ± 0.05		24.35	0
		ΔG^0_i (kJ/mol)	24.35 ± 0.35			
Y79X	Y79F	$[D]_{1/2}$ (M)	4.13			
		$-m$ (kJ/M/mol)	3.80 ± 0.02		17.84	−6.51
		ΔG^0_i (kJ/mol)	17.84 ± 0.82			
	Y79W	$[D]_{1/2}$ (M)	4.6	7.1		
		$-m$ (kJ/M/mol)	4.08 ± 0.04	6.78 ± 0.13	22.32	−2.03
		ΔG^0_i (kJ/mol)	18.86 ± 0.18	48.61 ± 0.08		
	Y79W	$[D]_{1/2}$ (M)	4.6	7.1		
		$-m$ (kJ/M/mol)	4.08 ± 0.04	6.78 ± 0.13	22.32	0
		ΔG^0_i (kJ/mol)	18.86 ± 0.18	48.61 ± 0.08		
W83L	Y79WW83L	$[D]_{1/2}$ (M)	3.00			
		$-m$ (kJ/M/mol)	3.62 ± 0.06		10.88	−11.44
		ΔG^0_i (kJ/mol)	10.88 ± 0.21			
	Y79WW83F	$[D]_{1/2}$ (M)	4.2	7.2		
		$-m$ (kJ/M/mol)	4.88 ± 0.02	4.76 ± 0.03	24.14	1.82
		ΔG^0_i (kJ/mol)	20.55 ± 0.10	33.70 ± 0.18		

Table V. *Thermodynamics Parameters of apoCopC and Its Mutants from GdnHCl-Induced Unfolding at pH 7.4, 25°C*

	Protein	Parameters	F (I/U)	I (U)	$<\Delta G^0_{element}>$ (kJ/mol)	$\Delta<\Delta G^0_{element}>$ (kJ/mol)
	apoCopC	$[D]_{1/2}$ (M)	1.55			
		$-m$ (kJ/M/mol)	16.16 ± 0.22		24.98	0
		ΔG^0_i (kJ/mol)	24.98 ± 0.31			
Y79X	Y79F	$[D]_{1/2}$ (M)	0.99			
		$-m$ (kJ/M/mol)	17.30 ± 0.39		17.04	−7.94
		ΔG^0_i (kJ/mol)	17.04 ± 0.38			
	Y79W	$[D]_{1/2}$ (M)	1.33			
		$-m$ (kJ /M/mol)	15.13 ± 0.11		20.16	−4.82
		ΔG^0_i (kJ/mol)	20.16 ± 0.13			
	Y79W	$[D]_{1/2}$ (M)	1.33			
		$-m$ (kJ/M/mol)	15.13 ± 0.11		20.16	0
		ΔG^0_i (kJ/mol)	20.16 ± 0.13			
W83X	Y79WW83L	$[D]_{1/2}$(M)	0.64			
		$-m$ (kJ/M/mol)	16.92 ± 1.19		10.75	−9.41
		ΔG^0_i (kJ/mol)	10.75 ± 0.74			
	Y79WW83F	$[D]_{1/2}$ (M)	1.16	1.54		
		$-m$ (kJ/M/mol)	17.79 ± 0.22	17.04 ± 0.73	23.58	3.42
		ΔG^0_i (kJ/mol)	20.65 ± 0.23	26.27 ± 1.32		

79W>Y79WW83L. The replacement of Trp83 with Phe and Leu induced a completely opposite effect, indicating that the aromatic ring of Trp83 was important in maintaining the hydrophobic core of apoCopC.

Discussion

CopC in the solution adopts a fold essentially constituted by two β sheets forming a Greek key β-barrel motif that involves nine strands, two of which are parallel; the others are all antiparallel. The protein contains the hydrophobic core in which a single Trp residue and the Tyr are located. In this study, we revealed the roles of Tyr and the unique Trp in apoCopC and the microenvironment around the two resides through far-UV CD spectra, acrylamide, and KI quenching experiments, fluorescence lifetime, and chemical denaturation.

In a quenching experiment, acrylamide only quenched usually considered only quenching the chromophore fluorescence buried deeply in the protein. However, KI seemed to quench the chromophore located in the protein surface with the close water environment. The data in Table III reveal that the degree quenched by acrylamide was significantly greater than that of KI. This phenomenon suggests that the Trp is deeply buried in protein. In addition, K_{SV} (Y79WW83L and Y79WW83F quenched by KI) was greater than K_{SV} (apoCopC, Y79F quenched by KI). This result shows that KI can access the Trp more easily when the Trp is located at the 79 position, further indicating that the environment around the position 83 is more hydrophobic than that around position 79 in mutants. This inference was also confirmed by fluorescence lifetime measurement. The lifetimes of Y79WW83L and Y79WW83F were larger than that of apoCopC and Y79F, suggesting that the extent of Tyr79 exposed in a hydrophilic environment was more enhanced compared with that of Trp83.

To assess the effects of the mutations on the fluorescence characteristics of the proteins, we analyzed their emission spectra using fluorescence spectroscopy. For Y79F, the exclusive Trp was located at the 83 position near the N-terminal domain of the protein. Maximum emission at any shift did not take place. However, in the exclusive Trp for Y79WW83L and Y79WW83F located at the 79 position near the C-terminal, the emission wavelength shifted from 320 to 328 and 331 nm, respectively. For Y79W, the Trp residue seemed to be situated under different environments, two Trps contributed to the florescence, and the maximum emission shifted from 320 to 325 nm. These phenomena suggest that the microenvironment around Trp83 was more hydrophobic than that around Tyr79 in apoCopC. These results agreed with the results of the quenching experiment.

Furthermore, the effects of mutation on the binding capacity of Cu(II) are manifested. Table I shows that the binding constants for mutants were almost unchanged. These results suggest that the binding ability is essentially affected. The NMR structure of apoCopC shows that the mutational amino acid residues are far away from the amino acid residues coordinated with Cu(II). Therefore, this local structure was almost unaffected by mutations.

Table IV shows that apoCopC, Y79F and Y79W unfolding was induced by urea with $<\Delta G^0_{element}>$ of 24.35, 17.84, and 22.32 kJ/mol, respectively. The $<\Delta G^0_{element}>$ of Y79F and Y79W were lower than that of apoCopC, namely, 6.51 and 2.03 kJ/mol, respectively. Similar phenomenon was observed from

the far-UV CD spectral [Fig. 1(A)]. Replacing Tyr79 with Phe increased β-sheet content more than that with Trp. The differences among the three proteins were the amino acid residue at the 79 position, which were Tyr, Trp, and Phe, respectively. The abilities of these proteins in forming hydrogen bonds decreased successively, in contrast to just opposite their hydrophobicity. Coincidentally, the sequence of decline of the β-sheet content and the decrement order of the $<\Delta G^0_{element}>$ were ascribed to the mutants, which agreed with the abilities of these proteins in forming H-bonds. These results suggest that the ability of the 79th amino acid to form H-bonds has a very important role in maintaining the structure of apoCopC. In addition, apoCopC contains a hydrophobic core, and Try79 and Trp83 are located in the core. The NMR structure of apoCopC[20] shows that Tyr79 interacts with Thr75 in the tyrosine corner[37] at the hydrophilic side chain outside the hydrophobic core through hydrogen bonds (Supporting Information Fig. S5A). When Tyr79 was replaced with Trp and Phe, the hydrophobicities of their side chains were larger than those of Tyr, resulting in a small torsion in the benzene ring of Trp and Phe compared with that of Tyr (Supporting Information Fig. S5B,C). The structures of mutants were obtained from Phyre.[38] Eventually, leading to the hydrogen bonds between Thr75 and Trp, and Phe were lost or reduced. Therefore, the stability of Y79F and Y79W decreased. Similar results were obtained from the unfolding induced by GdnHCl (Table V). In summary, the CD spectra and the stability of the proteins indicated that the hydrogen bond interactions between Tyr79 and Thr75 have an important role in stabilizing apoCopC.

The thermodynamic parameters for the unfolding of Y79W, Y79WW83L, and Y79WW83F induced by urea/GdnHCl are listed in Tables IV and V. Table IV shows that Y79W, Y79WW83L, and Y79WW83F unfolding was induced by urea with $<\Delta G^0_{element}>$ of 22.32, 10.88, and 24.14 kJ/mol, respectively. The $<\Delta G^0_{element}>$ of Y79WW83L was lower than that of Y79W, and the $\Delta<\Delta G^0_{element}>$ was 11.44 kJ/mol. However, the $<\Delta G^0_{element}>$ of Y79WW83F was higher than that of Y79W and the $\Delta<\Delta G^0_{element}>$ was 1.82 kJ/mol. Notably, the replacement of Trp83 with Phe and Leu induced a completely opposite effect on the $<\Delta G^0_{element}>$ of proteins compared with Y79W. When Trp83 was replaced by Phe, the possibility of the formation of H-bonds was lost. The hydrogen bond is an important force for maintaining the protein's specific, compact, and three-dimensional structure of proteins. The loss of hydrogen bonds would result in lower protein stability.[39] However, the $<\Delta G^0_{element}>$ of Y79WW83F induced by urea or GdnHCl all increased (Tables IV and V). In addition, the β-sheet content for Y79WW83F increased by 2% from the far-UV CD spectra [Fig. 1(B)]. This phenomenon suggests that Trp83 did not maintain the protein structure through hydrogen bonds. The NMR of apoCopC shows that the microenvironment around Trp83 was very hydrophobic and the hydrophobicity of Phe was larger than that of Trp. Thus, replacing Trp with Phe induced the Phe residue to reverse toward the interior of the hydrophobicity core, further forming a partial, more compact structure which increased the stability of Y79WW83F (Supporting Information Fig. S5D). The appearance of the intermediate of Y79WW83F also confirmed this inference. When Trp83 was replaced by Leu, hydrophobicity increased, but did not possess an aromatic ring. In addition, the volume of Leu was so small that a hydrophobic bond was not formed, resulting in the reduction of the $<\Delta G^0_{element}>$ reduced obviously (Supporting Information Fig. S5D). These results indicate that the aromatic ring of Trp83 is important in maintaining the hydrophobic core of apoCopC.

Interestingly, the unfolding of Y79WW83F shows a stable intermediate species whether urea or GdnHCl induced. This phenomenon is similar to the unfolding curve of CopC-Cu(II) induced by urea (25°C, pH 7.4).[1] CopC is a periplasmic copper chaperone protein that has a β-barrel fold and two metal-binding sites distinct for Cu(II) and Cu(I). One metal site is specific for Cu(I) and the other for Cu(II). The Cu(I) site is situated in a disordered loop near the C-terminus, whereas the N-terminus is a Cu(II) ligand.[17] The binding of Cu(II) increased the stability of the N-terminus, whereas the replacement of Trp83 with Phe formed a partial more compact structure in the N-terminus. This result may be due to the fact that the Y79WW83F intermediate resembles an equilibrium intermediate observed for CopC-Cu(II). In addition, recent research about I27 suggests that the mutated form of I27 causes a bend in the backbone structure, which leads to the formation of a more stable N-terminal structure probably through enhanced hydrophobic interactions.[40] The unfolding curve of the Y79W induced by urea also shows two transitions. The intermediate ascribed to the mutant was also observed for the pseudo-azurin structure, another protein with the same β-barrel fold as CopC. Equilibrium denaturation of Y74W apo-pseudoazurin demonstrated a multistate unfolding in urea, which resulted from the important role of the tyrosine corner in unfolding.[41] Interestingly, the replacement of Tyr79 in apoCopC with threonine, serine, or histidine resulted in proteins that could not be expressed (data not shown), suggesting that the interactions in the tyrosine corner are essential for the generation and/or maintenance of the integrity of the protein fold.

Conclusions

The investigation on the fluorescence properties of apoCopC and its mutants indicated that the

microenvironment around position 83 was more hydrophobic than that around position 79 in apoCopC. The important roles of Tyr79 and Trp83 in maintaining the stability of apoCopC were monitored by far-UV CD spectra and urea/GdnHCl-induced unfolding experiments. The results showed that the hydrogen bond interactions between Tyr79 and Thr75 have a critical role in stabilizing apoCopC. Furthermore, the aromatic ring of Trp83 is important in maintaining the hydrophobic core of apoCopC.

Materials and Methods

Materials

Potassium dihydrogen phosphate, potassium hydrogen phosphate and phosphoric acid, sodium chloride, Hepes (4-(2-hydroxyethyl)-1-piperazine-ethanesulfonic acid), guanidine hydrochloride, urea, potassium iodide, acrylamide, sodium dithionite, EDTA, $CuCl_2$ and other chemicals were all analytical grade reagents.

Methods

Site-directed mutagenesis. Point mutations were introduced into the CopC DNA using the TakaRa Mutan BEST Kit 401, and all reactions were carried out as suggested by the manufacturer. PET-20b-CopC was used as a template for the preparation of the Y79F and Y79W. A specific PCR fragment was prepared using the primer pairs Y79F (5′-CG GCA GGC ACC TGG AAG GTC GAT TG-3'), and (5′-T CAG AGG TGA GGC CGG GGT AAT CAC CAT G-3'), likewise Y79W (5′-TGG CGG GCA GTG TCT TCC GAT ACC CAC CCG-3′) and (5′-ATC GAC CTT GAA GGT GCC TGC CGT CAG AGG-3′). The double mutant was constructed by using PET-20b-W83L and PET-20b-Y79W DNA as template for Y79WW83L and Y79WW83F, respectively. Using the primers as follows: Y79WW83L (5′-ACG GCA GGC ACC TGG AAG GTC GAT TTG CG-3′) and (5′-CAG AGG TGA GGC CGG GGT AAT CAC CAT G-3′), Y79WW83F (5′-GTG TCT TCC GAT ACC CAC CCG ATT AC-3′) and (5′-TGC CCG GAA ATC GAC CTT CCA GGT GC-3′). In all cases, the presence of the specific mutation was verified by DNA sequence analysis, which was conducted by a commercial company.

Protein expression and purification. The methods employed for protein expression and purification have been described previously.[21] The target proteins were identified via 15% SDS-PAGE. After purification, the proteins were kept at -20°C, the stock protein solutions were conserved in 0.01*M* Hepes. Protein concentration was measured at 280 nm, using molar extinction coefficients at 280 nm of $6970M^{-1}cm^{-1}$ for apoCopC ; $5500M^{-1}cm^{-1}$ for (Y79F, Y79WW83L, Y79WW83F); and $11{,}000M^{-1}cm^{-1}$ for Y79W by a Hewlett Packard 8453 spectrophotometer.

The far-UV circular dichroism. Circular dichroism (CD) measurements were carried out on MOS 450 (BioLogic, France) spectropolarimeter continuously purged by N_2 and equipped with a temperature-control system. All spectra were the average of three scans with a step size of 0.2 nm and a band width of 1 nm. Far-UV spectra were recorded between 195 and 250 nm using 1-mm path length quartz cells. The protein concentration was 25 μ*M* in 2 m*M* Hepes, pH 7.4, at 25°C.

Copper binding measurements. A fresh stock solution of $CuCl_2$ and EDTA were prepared in distilled water. For copper binding experiments, A Cary Varian Eclipse fluorescence spectrophotometer was applied to record the protein fluorescence spectra. The excitation wavelength was set at 295 nm and the emission spectra were taken in the range of 300–450 nm. Both the excitation and emission slits were set at 5 nm.

Fluorescence lifetime measurement. Fluorescence lifetimes were collected by the time-correlated single-photon counting technique on an Edinburgh Analytical Instruments type nF-900 fluorometer. The excitation source was a flash lamp filled with hydrogen (0.4 atm) and operated at 40 kHz with approximately 6.86 kV across a 1 mm gap. Ludox HS-30 scattering solution was used to collect the instrument's response. The excitation (295 nm) and emission (320 nm) wavelengths were selected using monochromators. The sample concentrations were about 25 μ*M* in time-resolved experiments. All measurements were performed in 10 m*M* Hepes, pH 7.4, at 25°C. The fluorescence decay of the tryptophan was analyzed using a sum of exponentials: $I(t) = \sum B_i \exp(-t/\tau_i)$ where B_i and τ_i are the amplitude and lifetime, respectively. $I(t)$ was convoluted with the measured instrumental response and then compared with the experimental data by nonlinear least-squares methods.

Acrylamide and KI-quenching experiments. In the quenching experiments, aliquots of 1.5*M* quencher stock solution were added to protein solutions (2 μ*M*) to achieve the desired range of quencher concentration (0–0.05*M*). Furthermore, for KI-quenching experiments, few sodium dithionite should be added to prevent the formation of iodine. Excitation wavelength was set at 295 nm in order to excite tryptophan residues only and the emission spectrum was recorded in the range 300 nm to 450 nm. The decrease in fluorescence intensity was

analyzed by using the Stern–Volmer equation: $F_0/F=1+ K_{SV}[Q]$, where F_0 is the fluorescence of the protein in the absence of quenchers and F is the observed fluorescence at the concentration $[Q]$ of the quencher. K_{SV} is the collisional quenching constant which was determined from the slope of the Stern–Volmer plot at lower concentrations of quencher, whereas $[Q]$ represents molar concentration of quencher.

Chemical unfolding experiments. Urea/GdnHCl-induced unfolding of apoCopC and its mutants was performed, in 10 m*M* Hepes, pH 7.4, at 25°C. GdnHCl/urea stocks were prepared by dissolving solid denaturant in distilled water. In each GdnHCl denaturation experiment, every sample was titrated with GdnHCl from 0 to 4*M*, at a protein concentration of 2 μ*M*. Similarly, the concentration of urea was from 0 to 10*M*. All samples were incubated for 1 h before emission measurements. There was no time dependence in the reactions for incubation times between 30 min and 48 h.

Analysis of denaturation data. In this article, two state unfolding curves were analyzed by a linear extrapolation method. Three state unfolding curves were analyzed using the new model proposed by our group to obtain the values of the free energy of average structural element unfolding in water $<\Delta G^0_{\text{element}}(H_2O)>$ and the midpoint of transition $D_{1/2}$.[26]

The model was used to calculate the free energy change of protein unfolding. In this model, it is considered that proteins are composed of structural elements. The unfolding of a structural element obeys a two-state mechanism and the free energy change of the element can be obtained by a linear extrapolation method. The contribution of each structural element to the protein can be obtained by using linear extrapolation to zero denaturant concentration.

REFERENCES

1. Hussain F, Sedlak E, Wittung-Stafshede P (2007) Role of copper in folding and stability of cupredoxin-like copper-carrier protein CopC. Arch Biochem Biophys 467: 58–66.
2. Sticke DF, Presta LG, Dill KA, Rose GD (1992) Hydrogen bonding in globular proteins. J Mol Biol 226:1143–1159.
3. Myers JK, Pace CN (1996) Hydrogen bonding stabilizes globular proteins. Biophys J 71:2033–2039.
4. Mirsky AE. Pauling L (1936) On the structure of native denatured and coagulation proteins. Proc Natl Acad Sci USA 22:439–447.
5. Kauzmann W, Some factors in the interpretation of protein denaturation. In: Anfinsen CB, Anson Kenneth BaileyJohn ML, Edsall T, Eds. (1959) Advances in protein chemistry. Academic Press, New York and London. pp 1–63.
6. Tanford C (1962) Contribution of hydrophobic interactions to the stability of the globular conformation of proteins. J Am Chem Soc 84:4240–4247.
7. Pace CN, Shirley BA, McNutt M, Gajiwala K (1996) Forces contributing to the conformational stability of proteins. FASEB J 10:75–83.
8. Pace CN, Laurents DV, Erickson RE (1992) Urea denaturation of barnase: pH dependence and characterization of the unfolded state. Biochemistry 31:2728–2734.
9. Ma B, Elkayam T, Wolfson H, Nussinov R (2003) Protein–protein interactions: structurally conserved residues distinguish between binding sites and exposed protein surfaces. Proc Natl Acad Sci USA 100:5772–5777.
10. Chen Y, Barkley MD (1998) Toward understanding tryptophan fluorescence in proteins. Biochemistry 37: 9976–9982.
11. Killian JA, von Heijne G (2000) How proteins adapt to a membrane–water interface. Trends Biochem Sci 25: 429–434.
12. Arnesano F, Banci L, Bertini I, Thompsett AR (2002) Solution structure of CopC: a cupredoxin-like protein involved in copper homeostasis. Structure 10:1337–1347.
13. Zhang LY, Koay M, Maher MJ, Xiao ZG, Wedd AG (2006) Intermolecular transfer of copper ions from the CopC protein of pseudomonas syringae. Crystal structures of fully loaded Cu(I) Cu(II) forms. J Am Chem Soc 128:5834–5850.
14. Cha JS, Cooksey DA (1991) Copper resistance in pseudomonas syringae mediated by periplasmic and outer membrane proteins. Proc Natl Acad Sci USA 88:8915–8919.
15. Culotta VC, Klomp LWJ, Strain J, Casareno RLB, Krems B, Gitlin JD (1997) The copper chaperone for superoxide dismutase. J Biol Chem 272:23469–23472.
16. Arnesano F, Banci L, Bertini I, Mangani S, Thompsett AR (2003) A redox switch in CopC: an intriguing copper trafficking protein that binds copper(I) and copper(II) at different sites. Proc Natl Acad Sci USA 100: 3814–3819.
17. Djoko KY, Xiao ZG, Huffman DL, Wedd AG (2007) Conserved mechanism of copper binding and transfer. A comparison of the copper-resistance proteins pcoc from escherichia coli and CopC from pseudomonas syringae. Inorg Chem 46:4560–4568.
18. Koay M, Zhang LY, Yang BS, Maher MJ, Xiao ZG, Wedd AG (2005) CopC protein from pseudomonas syringae: intermolecular transfer of copper from both the copper(I) and copper(II) sites. Inorg Chem 44:5203–5205.
19. Silver S, Phung LT (1996) Bacterial heavy metal resistance: new surprises. Annu Rev Microbiol 50:753–789.
20. Arnesano F, Banci L, Bertini I, Felli IC, Luchinat C, Thompsett AR (2003) A strategy for the NMR characterization of type II copper(II) proteins: the case of the copper trafficking protein CopC from pseudomonas syringae. J Am Chem Soc 125:7200–7208.
21. Pang EG, Zhao YQ, Yang BS (2005) Fluorescence study on the interaction between apoCopC and cupric. Chinese Sci Bull 50:2302.
22. Zheng XY, Pang EG, Li HQ, Zhao YQ, Yang BS (2007) The role of cupric in maintaining the structure of CopC. Chinese Sci Bull 52:743–747.
23. Sze CM, Khairallah GN, Xiao ZG, Donnelly PS, O'Hair RA, Wedd AG (2009) Interaction of cisplatin and analogues with a met-rich protein site. J Biol Inorg Chem 14:163–165.
24. Mei G, Di Venere A, Campeggi FM, Gilardi G, Rosato N, De Matteis F, Finazzi-Agrò A (1999) The effect of pressure and guanidine hydrochloride on azurins mutated in the hydrophobic core. Eur J Biochem 265: 619–626.

25. Pace CN, Grimsley GR, Scholtz JM, Denaturation of proteins by urea and guanidine hydrochloride. In: Fersht AR, Ed. (2008) Protein science encyclopedia. Wiley-VCH, Hoboken, NJ, pp 45–69.
26. Yang BS, Song Z, Zheng XY, Zhao YQ (2012) Stability of proteins with multi-state unfolding behavior. Sci China Chem 55:1351–1357.
27. Burstein EA, Vedenkina NS, Ivkova MN (1973) Fluorescence and the location of tryptophan residues in protein molecules. Photochem Photobiol 18:263–279.
28. Phillips SR, Wilson LJ, Borkman RF (1986) Acrylamide and iodide fluorescence quenching as a structural probe of tryptophan microenvironment in bovine lens crystallins. Curr Eye Res 5:611–620.
29. Lehrer S (1971) Solute perturbation of protein fluorescence. Quenching of the tryptophyl fluorescence of model compounds and of lysozyme by iodide ion. Biochemistry 10:3254–3263.
30. Eftink MR, Ghiron CA (1976) Exposure of tryptophanyl residues in proteins. Quantitative determination by fluorescence quenching studies. Biochemistry 15:672–680.
31. Eftink MR, Ghiron CA (1981) Fluorescence quenching studies with proteins. Anal Biochem 114:199–227.
32. Liepinsh E, Otting G (1994) Specificity of urea binding to proteins. J Am Chem Soc 116:9670–9674.
33. Makhatadze GI, Privalov PL (1992) Protein interactions with urea and guanidinium chloride: a calorimetric study. J Mol Biol 226:491–505.
34. Pace CN, Determination and analysis of urea and guanidine hydrochloride denaturation curves. In Hirs CHW, Timasheff SN, Eds. (1986) Methods in enzymology. Academic Press, Orlando, Florida. pp 266–280.
35. Timasheff SN (1992) Water as ligand: preferential binding and exclusion of denaturants in protein unfolding. Biochemistry 31:9857–9864.
36. Tsai J, Gerstein M, Levitt M (1996) Keeping the shape but changing the charges: a simulation study of urea and its iso-steric analogs. J Chem Phys 104:9417–9430.
37. Hemmingsen JM, Gernert KM, Richardson JS, Richardson DC (1994) The tyrosine corner: a feature of most greek key β-barrel proteins. Protein Sci 3:1927–1937.
38. Kelley LA, Sternberg MJ (2009) Protein structure prediction on the web: a case study using the phyre server. Nat Protoc 4:363–371.
39. Anderson DE, Hurley JH, Nicholson H, Baase WA, Matthews BW (1993) Hydrophobic core repacking and aromatic–aromatic interaction in the thermostable mutant of t4 lysozyme ser 117 → phe. Protein Sci 2: 1285–1290.
40. Yagawa K, Yamano K, Oguro T, Maeda M, Sato T, Momose T, Kawano S, Endo T (2010) Structural basis for unfolding pathway-dependent stability of proteins: vectorial unfolding versus global unfolding. Protein Sci 19:693–702.
41. Jones S, Reader JS, Healy M, Capaldi AP, Ashcroft AE, Kalverda AP, Smith DA, Radford SE (2000) Partially unfolded species populated during equilibrium denaturation of the β-sheet protein Y74W apo-pseudoazurin. Biochemistry 39:5672–5682.